Wideband Ultrasonic Spectroscopy Part II

ULTRASONIC ATTENUATION OF PARTIALLY SINTERED CERAMICS: EXPERIMENTAL ANALYSIS

Nagraj Kulkarni* and Brij Moudgil*
Department of Materials Science & Engineering
University of Florida
Gainesville, Fl

Mahesh Bhardwaj*
Ultran Labs
Boalsburg, PA

ABSTRACT

Ultrasonic velocity and relative attenuation measurements of colloidally processed alumina were carried out. Upto a relative density of 70-75 %, low frequency (5 MHz) velocities were sensitive to the green microstructure. At higher densities velocities showed a linear behavior. Relative attenuation paths for partially sintered samples having varying green microstructures were distinctively different.

INTRODUCTION

The control of ceramic microstructure during its evolution from a green to a fully densified state is essential for obtaining a defect free product. Normal methods of quantification include microstructural and mechanical analysis. Generally, most characterization techniques are destructive and are often time consuming. In most cases attention is devoted towards characterization of fully densified structures, since partially sintered structures are difficult to handle on account of their fragile nature. The understanding of porous microstructures and their evolution from a porous to a fully densified state would be essential for developing effective on-line quality control systems. Non-destructive techniques such as ultrasonics have the capability of analyzing not only mechanical properties but microstructural properties as well [1].

The conventional ultrasonic measurements carried out are those of velocity and attenuation. Ultrasonic velocity is considered as more of a macroscopic property and is mainly used for determination of elastic properties [2-4], although in many cases it may be used to

---

* Member, American Ceramic Society

determine microstructural changes. Ultrasonic attenuation measurements are very sensitive to the microstructure and can depend on a variety of parameters such as the volume fraction and nature of porosity, grains, second phases, etc. Theoretical treatment of scattering due to various microstructural features in a material is complex. A number of significant contributions have been made in the past towards understanding scattering from grains and from pores or inclusions of specific geometry of which a notable contribution is the correlation between grain size distributions and attenuation measurements [1]. However most of the treatments are devoted to independent scattering models of densified structures. Understanding the attenuation of porous ceramics would require multiple scattering models in which scattering due to interaction between pores has to be considered. Although a number of significant contributions have been made in this direction [3,5] correlation with experimental data for higher volume fractions of porosity is difficult to obtain. This could be due to the complex nature of porosity in partially sintered structures where pores are generally interconnected and can be of complex shapes, sizes and distributions. Empirical approaches can provide some valuable insights in understanding the attenuation of partially sintered structures. An important observation made by Baaklini, et al. [6] is the relative sensitivity of attenuation measurements to density, pore shape and size of hot pressed silicon nitride. A continuous evaluation of attenuation measurements at various stages of densification could provide significant information about the state of microstructural evolution. In order to accomplish this, attenuation measurements were carried out on slip cast alumina samples at various stages of densification.

EXPERIMENTAL PROCEDURES

The experimental details including materials and procedures are given below.

Materials: High purity alpha alumina powder* (AKP-30) of density 3.98 g/cc was used for this

---

* Sumitomo Chemical America, Inc., NY

study.

Reagent grade chemicals, including HNO_3, KOH and KNO_3, to adjust pH and ionic strength, were obtained from Fisher Scientific Co.

Particle Characterization

Particle size: Particle size distribution was measured using a light scattering technique*. The mean particle size was measured to be 0.49 microns.

Surface Area: The powder specific surface area** (multipoint BET) measured using nitrogen gas adsorption was 10 m^2/gm.

Surface charge: The surface charge of the alumina powder was measured by the ESA*** (electrokinetic sonic amplitude) technique. In this technique, the ESA of a 2 vol.% suspension of alumina was measured at constant ionic strength (0.005 M KNO_3). The ESA measurements were then converted into the zeta potential using the well known Smoluchowski equation, along with an additional inertial term [7,8].

Rheological measurements: The viscosity of the various suspensions was measured, as a function of shear rate, using a Brookfield splindle type digital viscometer.

Preparation of green samples: Various colloidal suspensions of alumina were prepared at different pH's (3.5 to 11.5). The solids loading of the suspensions was maintained at 40 vol%. The suspensions were sonicated to break apart the soft agglomerates and stirred with a high speed stirrer for adequate mixing. Green samples were prepared by slip casting. This was done by pouring the above suspensions into plastic rings set on absorbent plaster blocks. The cylindrical specimens thus prepared were approximately 26 mm in diameter and 6-8 mm in

---

* Model CAPA-700, Horiba Instruments, Inc., Irvine, CA

** Model OS-7, Quantachrome Corp., Syosett, NY

*** ESA-8000 System, Matec Applied Sciences, Hopkinton, MA

thickness.

Methods

Characterization of Green Samples

Mercury Porosimetry: Mercury Porosimetry* was used to measure the pore size distribution of green samples. The green density of the samples was then calculated from the total measured porosity.

Archimedes density: The green density, as well as the open and closed porosity of the samples was measured by the Archimedes technique. To impart sufficient strength for such measurements, the green samples were heat treated at 700°C for 2 hrs. The green density was not expected to change due to this treatment since the formation of interparticle contacts during the initial stages of sintering does not cause densification.

Sintering: The green samples prepared above were sintered at temperatures of 1200, 1350 and 1500°C for times varying from 1-60 hrs. A wide range of samples with varying densities and microstructures were thus generated.

Characterization of sintered samples

Archimedes: The sintered samples were characterized for porosity and density by the Archimedes technique. The densities reported are expressed as percentages of the theoretical density of 3.98 g/cc.

SEM analysis: SEM** (scanning electron microscopy) was used to characterize the microstructure of the samples.

Ultrasonic Analysis

Ultrasonic attenuation: In this work, the relative attenuation was measured by a different

---

* Model SP-100, Quantachrome Corp., Syosett, NY

** JEOL 35 CF, JSM 6400

technique than those described previously by other authors [9,10] for frequencies ranging from 5-30 MHz. Broad band Lambda transducers were used for this purpose [11,12] and clear fused quartz (CFQ) was used as a reference. This technique has been successfully used by Bhardwaj, et al. [13] for the analysis of ceramic superconductors. In this technique, the test material is excited with special transducers (λ series - Ultran Labs, PA), which have a very broad frequency spectrum analogous to "white" spectra in optical spectroscopy. Thus the material's incident frequency response selection can be evaluated over a relatively large composition of frequencies. This method uses a reference ultrasonic spectrum obtained by applying wideband transducers in direct transmission mode from a 1.0 cm thick optically flat and polished clear fused quartz (CFQ). Once the reference spectrum has been generated, similar spectra is obtained from test materials by sandwiching them between the transmitting and receiving transducers. Assuming that the reference spectrum corresponds to input frequency components, subtraction of test material's spectra from the reference spectrum establishes the relative frequency dependence of ultrasonic attenuation as a function of various material characteristics. It is important that once the reference spectrum from the CFQ has been established, the pulser, amplifier or FFT mechanism settings are not altered during data acquisition.

Samples for ultrasonic analysis were sufficiently smooth and flat for efficient ultrasound transmission. A Fast Fourier Transform was done to display the signal in the form of its frequency components. Both the ultrasonic velocity and attenuation were measured by sandwiching the top and bottom surfaces of the cylindrical samples between the transducers, so that the direction of ultrasound propagation was along the longitudinal axis of the cylinder.

RESULTS AND DISCUSSION

In order to use Ultrasonics for the characterization of ceramics through all the stages of microstructural evolution, from the green to the sintered state, it was initially necessary to prepare

green ceramics having controlled microstructures. The colloidal processing route (slip casting) was chosen as the technique for preparation of green ceramics [14]. The variable used for controlling the green properties was the pH of the colloidal suspension which in turn affects the surface charge or the zeta potential of the particles [7].

Green samples were sintered in air at various temperatures and times so as to obtain a wide range of densities and microstructures. The sintered samples were characterized for density, open and closed porosity by the Archimedes technique and for the microstructure by SEM (scanning electron microscopy). Ultrasonic velocity and attenuation measurements were carried out to determine the acoustic properties of various samples.

Characterization of Sintered Samples

The densification behavior of green bodies at various times and temperatures is illustrated in Figure 1. It is apparent that the green samples made from well dispersed suspensions (pH 4.0) have a higher densification rate and reach theoretical density at lower temperatures and times compared to samples made from partially flocculated suspensions (pH 10.5). The partially flocculated samples develop a higher fraction of closed pores at much lower densities as compared to the dispersed samples.

Ultrasonic Velocity

The longitudinal ultrasonic velocities for the various samples as a function of density are shown in Figure 2. It is seen that after a relative density of about 70 %, the velocities for all the samples show a linear behavior and fall within a narrow band. The higher rate of velocity increase for the well dispersed sample is evident (Table 1). This is consistent with the higher densification rate observed for these samples. The velocity paths for the different sets of green and partially sintered samples are different below a relative density of about 70 % and are strongly dependent on their green microstructures. The longitudinal and shear velocities exhibit

a similar pattern of behavior with increase in densities for various samples. Longitudinal velocities are about 1.5-1.7 times the shear velocities for the samples used in this study.

Elastic Moduli

The determination of elastic moduli using ultrasound offers unique advantages over standard mechanical tests both in terms of accuracy and time. By proper design of the test specimen, the different elastic constants can be determined [2-4] using various ultrasonic velocity measurements. If one assumes conditions of isotropy, the velocity-elasticity relations are straightforward and can be obtained from longitudinal and shear ultrasonic velocity measurements. These relations are given below.

$$E = V_l^2.\rho.(1+\sigma)(1-2\sigma)/(1-\sigma)$$

$$G = V_t^2.\rho$$

$$S = V_s^2.\rho_s$$

$$\sigma = (1-2b^2)/(2-2b^2), \text{where } b = V_t/V_l$$

$$K = E/[3(1-2\sigma)]$$

where,

V_l = Longitudinal wave velocity, m/s; V_t = Shear wave velocity, m/s; V_s = Surface wave velocity, m/s; E = Young's Modulus, Pa; G = Shear Modulus, Pa; S = Surface Modulus, Pa; K = Bulk Modulus, Pa

These relations were used to calculate the various moduli. The variation of Young's modulus with density is shown in Figure 3. The increase in modulus with density is more gradual if compared with the corresponding velocity increase with density. The bulk and shear moduli showed a similar kind of behavior. Figure 4 shows the variation of Poisson's ratio with density for samples having different green densities. The Poisson's ratio appears to fall within a band of 0.15 to 0.25 with a very gradual increase to the upper limit for higher density samples. As

seen from the figure, the experimental error in determining the Poisson's ratio is relatively large. Green, et al. [15] have reported a similar result. This is not surprising, since it is a small quantity dependent on differences of the other elastic properties and hence quite sensitive to errors in them [16].

Ultrasonic Attenuation Measurements

The frequency spectrum of a 1 cm thick clear fused quartz is shown in Figure 5. The relative attenuation for various samples was obtained by subtracting from the frequency components of the reference CFQ and these are shown in Figures 6 and 7 respectively as a function of frequency. The relative attenuation for three different frequencies are illustrated in Figures 8 and 9. It is observed from Figure 6 that:

a. The relative attenuation instead of decreasing with the decreasing porosity actually showed an increase. This is seen for the graphs of the samples having relative densities of 63.4 % and 76.1 %.

b. The samples having relative densities of 82.2 % and 95.5 % had lower attenuation than the above two samples. However, again it was seen that the sample with density of 82.2 % had a lower attenuation than the 95.5 % dense sample. A similar pattern of behavior is seen in Figure 7 for samples with densities of 62 and 63.9 % and those with 78.8 and 94.8 %.

Baaklini et al. [6] have reported a 150 % increase in the mean attenuation coefficient for a 1.97 % increase in density for samples of silicon nitride. However, it should be noted that they worked with extremely high frequencies (60-160 MHz) for samples with high densities (90-98 %), compared to the lower frequencies (10-30 MHz) and densities (60-90 %) encountered in the present study. Assuming that the longitudinal ultrasonic velocities for their silicon nitride samples ranged from 11,000 to 12,000 m/s, the wavelengths employed by them would range from

approximately 70 to 200 microns. The theory of ultrasonic grain scattering for dense materials is generally studied in three different regimes in which the frequency and grain size dependence of the attenuation is different. Depending upon the value of $\lambda/\bar{D}$ (λ is the wavelength and $\bar{D}$ the average diameter of the grains or dominant scatterer), these are the Rayleigh, Intermediate, Stochastic and Diffusive regions. The theory of scattering in these regions for polycrystalline materials has been considered by Papadakis [1]. The region of interaction in the work of Baaklini, et al. would correspond to the Rayleigh region ($\lambda > 2\pi\bar{D}$), since the dominant scatterers were shown to be the small amount of pores (having median diameters from 2-4 microns) in their samples. However, for partially sintered alumina ceramics as in the present work, multiple Rayleigh scattering is expected to occur considering the proximity of the pores, if one assumes the pores (~ 0.5 μm) to be the dominant scatterer. The contribution from grain boundaries (mean grain size from 1-5 microns for polycrystalline alumina) towards scattering for the frequencies employed in the present work is expected to be negligible compared to that from the pores. Besides the difference in scattering mechanisms, the relative attenuation and not the absolute attenuation was measured in this work, hence, a comparison with Baaklini's work is not possible.

It appears that, for the partially sintered samples, besides the total volume fraction of the porosity, the tortuosity of the pore-grain boundary interface, the size, shape, connectivity and distribution of the pores may also have a significant contribution. The increase in attenuation for the two partially sintered samples (63.4 and 76.1 %) (Figure 6) could be attributed to these factors.

The attenuation graphs for the samples having green density of 62.9 % have a lower slope and are much smoother as compared to those with green density of 53.9 %. This is expected since to begin with, the green partially flocculated samples had rather inhomogeneous

packing as compared to the dispersed samples.

In the second observation (b), the attenuation difference between the two samples having densities 82.2 and 95.5 % is not very significant. Still, this difference could again be attributed to microstructural changes occurring during the later stages of sintering such as grain growth, increase in the fraction of closed pores, etc. Beyond a density of about 80 % the low frequency attenuation measurements do not seem to be sensitive enough to detect microstructural variations due to grain scattering for the samples with the same green density. This is expected since the grain size of alumina ceramics is of the order of a few microns. Higher frequencies (possibly in GHz for alumina) would be required for such analyses [17].

However, when comparing the relative attenuations of samples with different green densities, the low frequency attenuation measurements are seen to be very sensitive even at high densities (> 90 %). It is seen from Table 2 that the relative attenuations for the partially flocculated and dispersed samples are clearly different for the range of densities studied in this work. It has been shown by Evans, et al. [18] that the attenuation is affected mostly by the dominant scatterers present in the ceramic. At low densities, due to the higher pore sizes the relative attenuation of the partially flocculated samples is seen to be higher. At intermediate densities, however, the dispersed samples have higher attenuations. This could be due to the complex microstructure existing during the intermediate stages of sintering. At high sintered densities, the partially flocculated samples show higher attenuations. This can be attributed to the presence of a few large size, stable pores present [19] in the partially flocculated samples. Large grains present in these samples may also aid in increasing the attenuation.

CONCLUSIONS

The velocity paths for various samples upto a relative density of 70-75% were unique and were a strong function of the initial green microstructure. At higher densities, velocity paths for

all samples fell in a narrow band and were independent of the prior history of the samples. The linear velocity-density relationship at higher densities was evident. The isotropic Young's, shear and bulk modulus followed a pattern similar to the velocity. However, the increase in the moduli at low densities (< 75 %) was not as exaggerated as the corresponding increase in ultrasonic velocities.

The relatively low frequency attenuation measurements (5-30 MHz) carried out in this work were sensitive to microstructural changes in the partially sintered samples. The attenuation paths for partially flocculated and dispersed samples were studied at four different frequencies as a function of density and these were unique. Thus the effect of the prior history and processing of these samples was reflected in the attenuation measurements. For samples that had undergone little densification as well as for samples that had almost densified (> 90 %), the partially flocculated samples showed much higher attenuations. This was attributed to the larger size of the dominant scatterers (pores) present in the partially flocculated samples. At intermediate densities, it was observed that the attenuation was a strong function of the complex microstructure existing in samples during the intermediate stages of sintering and did not monotonically decrease with an increase in density. Within samples having the same green density, the low frequency attenuation measurements (5-30 MHz) were not sensitive for samples having higher sintered densities (> 85 %). It is expected that high frequency attenuation measurements would be more sensitive to microstructural changes in these samples. Proper quantification of the microstructure during various stages of sintering would be necessary to properly account for the observed attenuation behavior.

ACKNOWLEDGEMENTS

Two of the authors (N. Kulkarni and B. M. Moudgil) acknowledge the National Science Foundation (MSS 8821815) for the financial support of this work.

REFERENCES

1. E. P. Papadakis, "Ultrasonic Attenuation Caused by Scattering in Polycrystalline Media," pp. 269-328 in Physical Acoustics: Principles and Methods," Vol. IV-Part B. Edited by W. P. Mason, Academic Press, NY, 1968.
2. A. B. Bhatia, Ultrasonic Absorption, Dover Publications, NY, 1967.
3. R. Truell, C. Elbaum and B. B. Chick, Ultrasonic Methods in Solid State Physics, Academic Press, NY, 1969.
4. E. Schreiber, O. L. Anderson and N. Soga, Elastic Constants and Their Measurement, pp. 1-33, McGraw-Hill, NY, 1973.
5. K. Goebbels, "Structural Analysis by Scattered Ultrasonic Radiation," pp. 87-157 in Research Techniques in Nondestructive Testing, Vol. 4. Edited by R. Sharpe, Academic Press, London, 1980.
6. G. Y. Baaklini, E. R. Generazio and J. D. Kisor, "High-Frequency Ultrasonic Characterization of Sintered Silicon Carbide," J. Am. Ceram. Soc., **72** [3], 383-87 (1989).
7. R. J. Hunter, Foundations of Colloid Science, Vols. 1 and 2, Oxford Univ. Press, Oxford, U.K., 1985.
8. R. W. O'Brien, "Electro-acoustic effects in a Dilute Suspension of Spherical Particles," J. Fluid Mech., 190, pp. 71-86, 1988.
9. E. P. Papadakis, "Ultrasonic Velocity and Attenuation: Measurement Methods with Scientific and Industrial Applications," pp. 277-374 in Physical Acoustics: Principles and Methods," Vol.XII. Edited by W. P. Mason and R. N. Thurston, Academic Press, NY, 1976.
10. E. R. Generazio, "The Role of the Reflection Coefficient in Precision Measurement of Ultrasonic Attenuation," pp. 995-1004, Materials Evaluation, 43, July 1985.
11. J. A. Brunk, C. J. Valenza and M. C. Bhardwaj, "Applications and Advantages of Dry Coupling Ultrasonic Tansducers for Materials Characterization and Inspection," pp. 221-237 in Acousto-Ultrasonics, Theory and Applications. Edited by J. C. Duke, Jr., Plenum Press, NY, 1988.
12. M. C. Bhardwaj, "Fundamental Developments in Ultrasonics for Advanced NDC," pp. 472-527 in NDT of High-Performance Ceramics, Conference Proceedings, Boston, MA, Aug. 25-27, 1987. Published by the American Ceramic Society, OH.
13. M. C. Bhardwaj, K. Trippett and A. S. Bhalla, "Microstructure Characterization of Superconductors by Wideband Ultrasonic Spectroscopy," pp. 1-10 in Superconductivity and Ceramic Superconductors, Proceedings of the First International Ceramic Science and Technology Congress, Anaheim, CA. Edited by K. M. Nair, Am. Cer. Soc. Westerville, OH, 1990.
14. F. F. Lange, "Powder Processing Science and Technology for Increased Reliability," J. Am.Ceram. Soc., **72** [1] 3-15 (1989).
15. D. J. Green, C. Nader and R. Brenzy, "The Elastic Behavior of Partially-Sintered Alumina," pp. 345-56 in Ceramic Transactions, Vol. 7. Edited by C. A. Handwerker, J. E. Blendell and W. A. Kaysser, American Ceramic Society, Westerville, OH, 1989.
16. R. W. Rice, "Microstructure Dependence of Mechanical Behavior," pp. 200-369 in Treatise on Materials Science and Technology, Vol. 11. Edited by R. K. MacCrone, Academic Press, NY, 1977.
17. W. A. Simpson, Jr. and R. W. McClung, "Quantitative Attenuation Techniques for Materials Characterization," Materials Evaluation, **49** [11] 1409-1413 (1991).
18. A. G. Evans, B. R. Tittmann, L. Ahlberg, B. T. Khuri-Yakub and G. S. Kino, "Ultrasonic Attenuation in Ceramics," J. Appl. Phys.,**49** [5] 2669-2679, May 1978.

19. B. J. Kellet and F. F. Lange, "Thermodynamics of Densification: I, Sintering of Simple Particle Arrays, Equilibrium Configurations, Pore Stability, and Shrinkage," J. Am. Ceram. Soc. **72** [5] 725-34 (1989).

LIST OF FIGURES

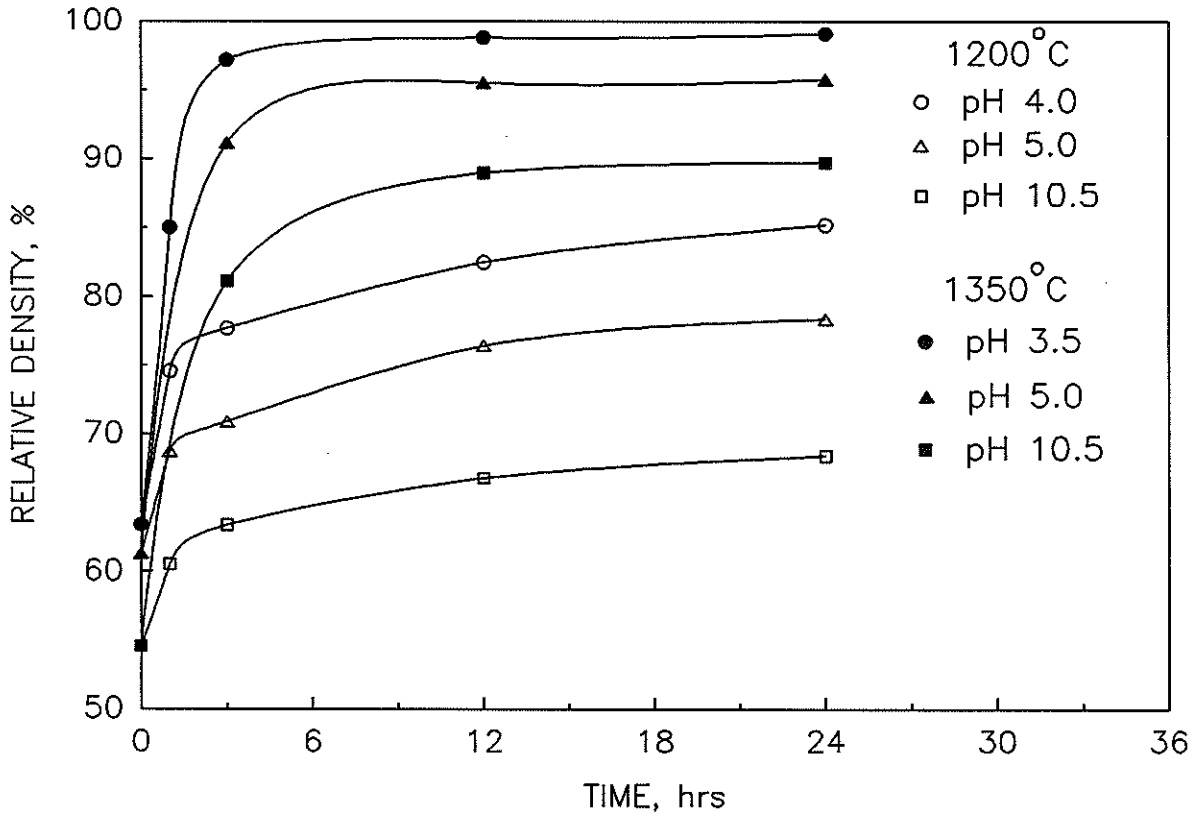

Figure 1. Densification behavior of green slip cast samples sintered at various temperatures and times.

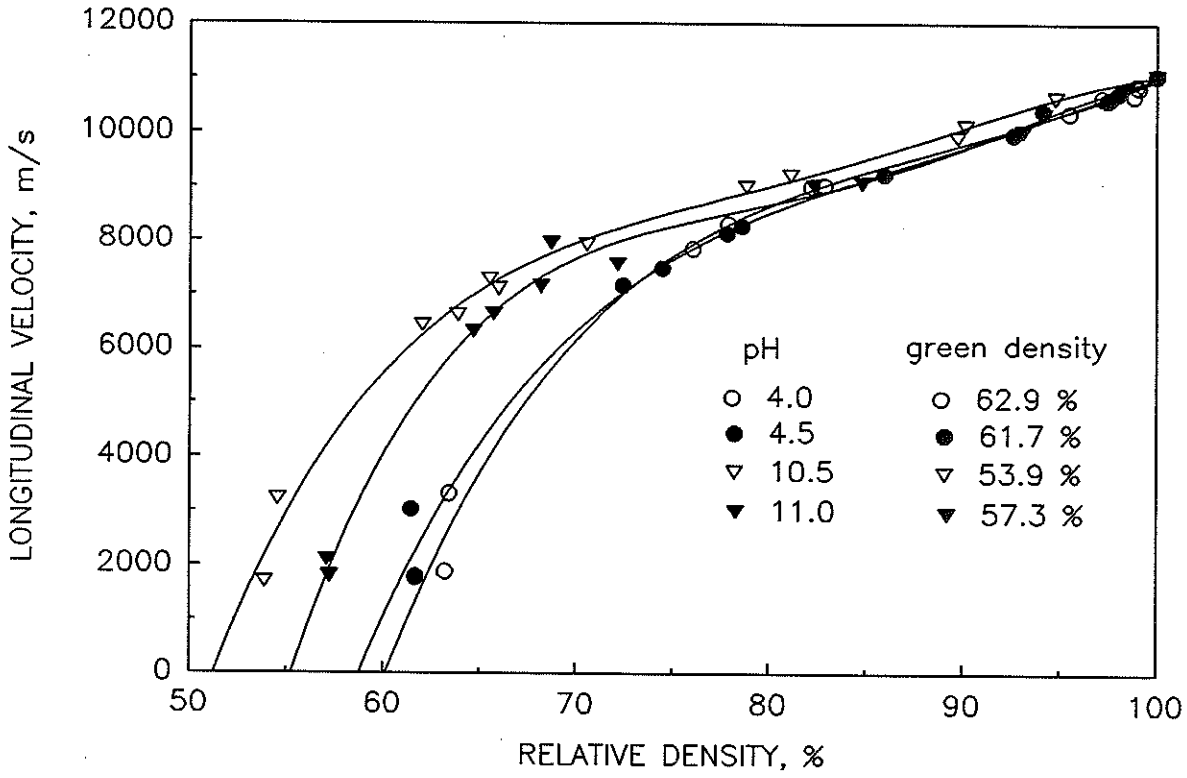

Figure 2. Variation of longitudinal velocity with percentage relative density for samples having different green densities.

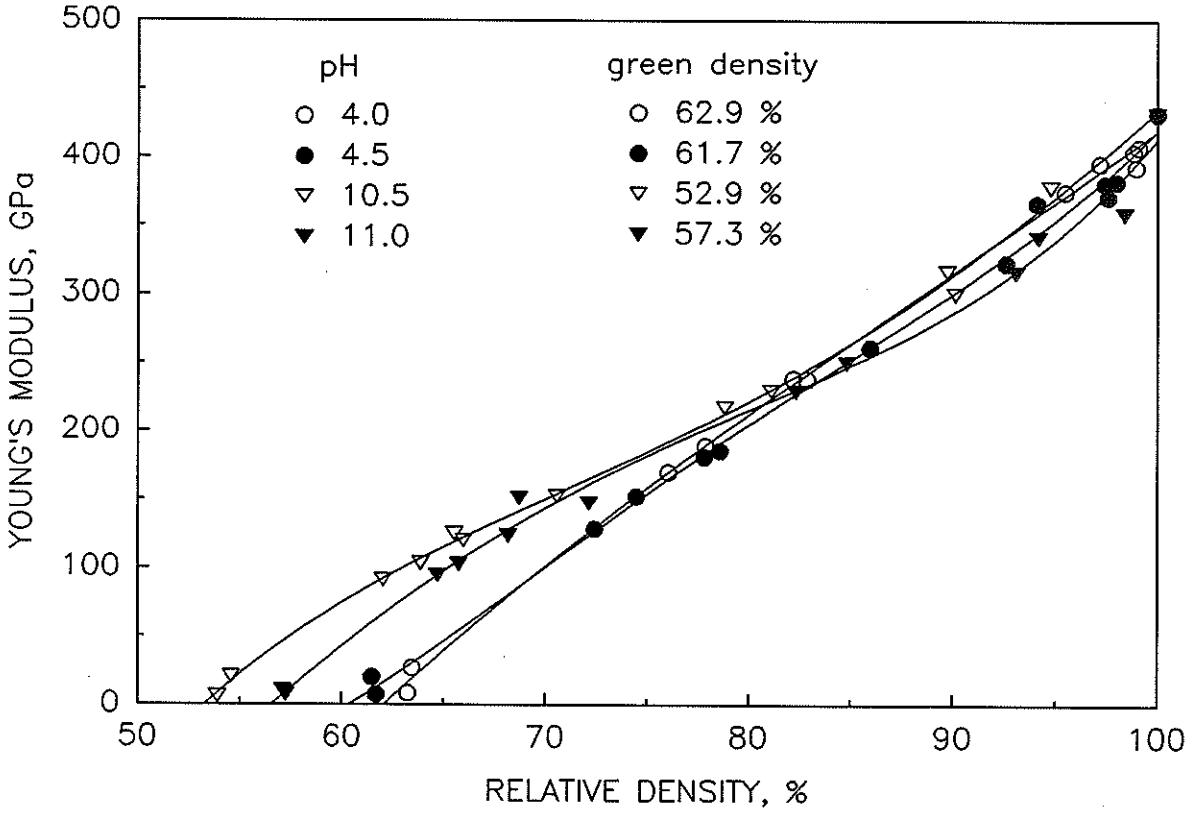

Figure 3. Young's modulus of elasticity as a function of percentage relative density.

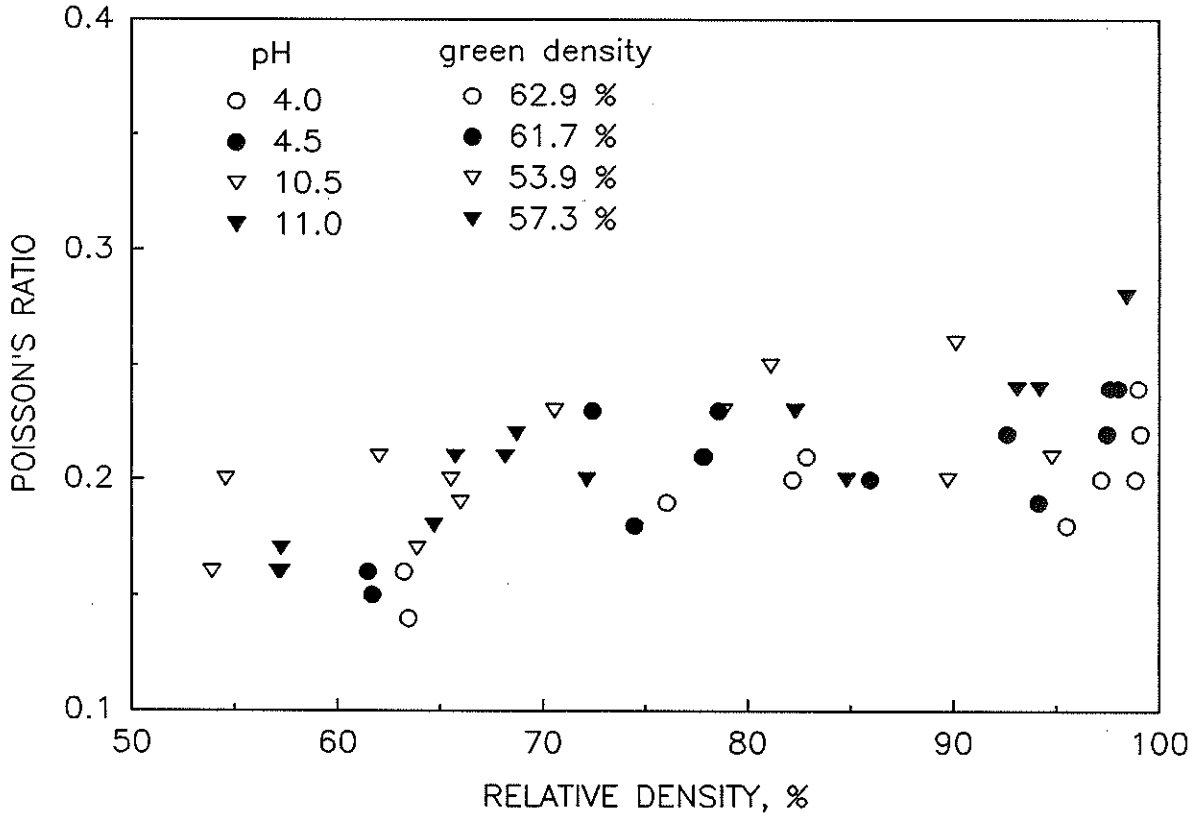

Figure 4. Poisson's ratio as a function of percentage relative density.

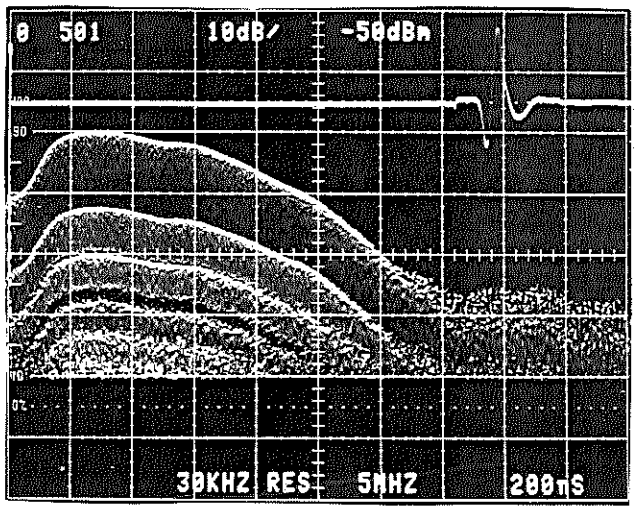

Figure 5. Time and Frequency Domain analysis of clear fused quartz (CFQ). Time Domain- Horizontal trace. Scale- Horizontal : 200 ns/div. Frequency Domain- Central envelope. Scale- Horizontal : 30 KHz/div. Vertical : 10 dB/div.

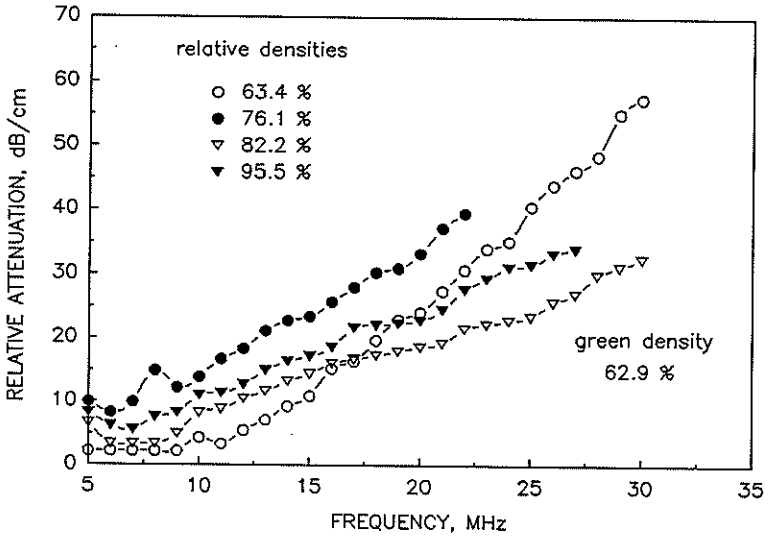

Figure 6. Relative attenuation as a function of frequency for samples having green densities of 62.9 %.

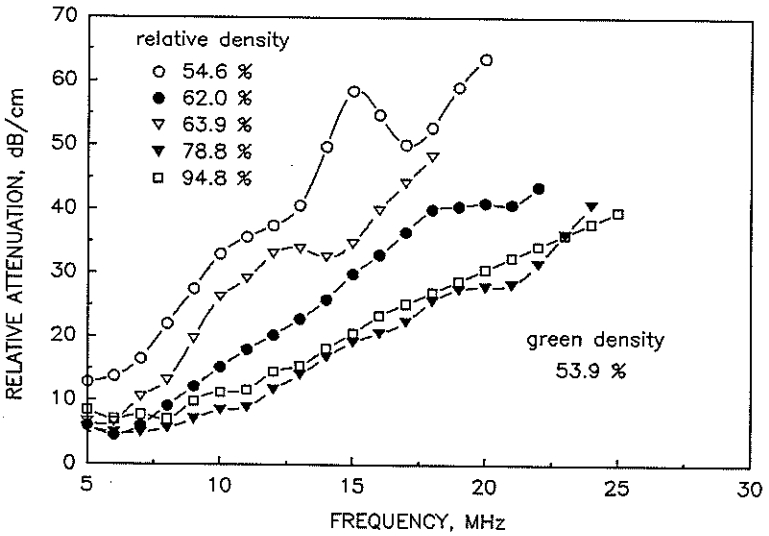

Figure 7. Relative attenuation as a function of frequency for samples having relative densities of 53.9 %.

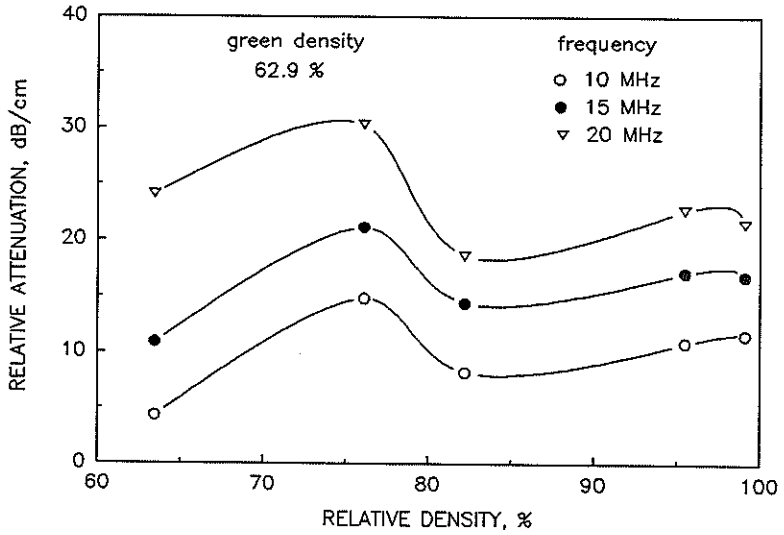

Figure 8. Relative attenuation for samples sintered to various densities but having the same green density of 62.9 %. The relative attenuation is plotted at three different frequencies.

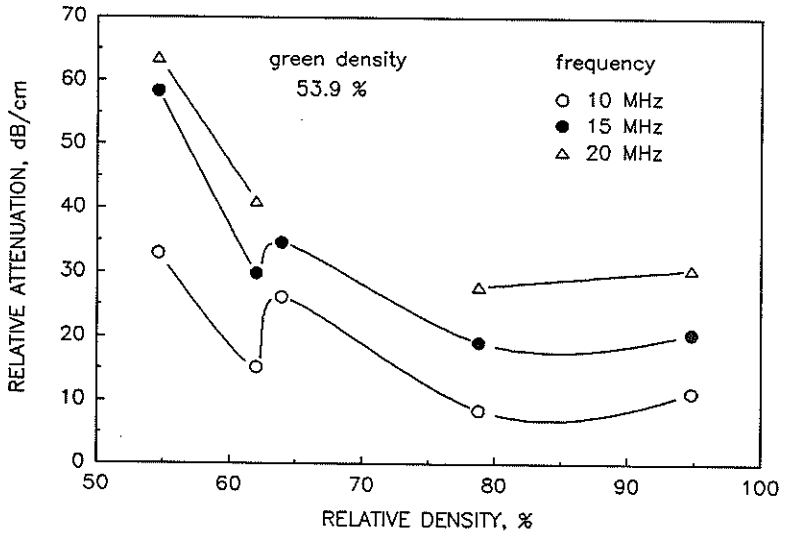

Figure 9. Relative attenuation for samples sintered to various densities but having the same green density of 53.9 %. The relative attenuation at three different frequencies is given.

LIST OF TABLES

Table 1. Ultrasonic velocities of sintered samples. (a) dispersed (b) partially flocculated

(a)

Sintering		Dispersed Samples (pH 4)		
Temp. (°C)	Time (hrs.)	Density (%)	Longitudinal Velocity (m/s)	Shear Velocity (m/s)
700	2	63.4	3318	2148
1200	1	76.1	7846	4862
1200	3	77.9	8312	5013
1200	12	82.2	9008	5513
1200	24	82.9	9027	5467
1350	1	95.5	10366	6452
1350	3	97.2	10656	6531
1350	12	98.8	10690	6541
1350	24	99.1	10844	6517
1500	3	99	10870	6335

(b)

Sintering		Partially Flocculated (pH 10.5)		
Temp. (°C)	Time (hrs.)	Density (%)	Longitudinal Velocity (m/s)	Shear Velocity (m/s)
700	2	54.6	3220	1976
1200	1	62	6430	3904
1200	3	63.9	6620	4167
1200	12	66	7102	4376
1200	24	65.5	7281	4479
1200	60	70.6	7928	4699
1350	1	78.8	9005	5298
1350	3	81.1	9214	5343
1350	12	90.1	10121	5757
1350	24	89.7	9914	6078
1500	3	94.8	10640	6426

Table 2. Comparison of relative attenuation of partially flocculated and dispersed samples.

Density (%)	State of Dispersion	Relative Attenuation (dB/cm)			
		5 MHz	10 MHz	15 MHz	20 MHz
62.0	flocculated*	6.1	15.2	29.8	41.0
63.4	dispersed	2.2	4.3	10.9	24.1
78.8	flocculated*	5.6	8.5	19.1	27.8
76.1	dispersed	9.9	14.8	21.1	30.3
94.8	flocculated*	8.4	11.3	20.5	30.6
95.5	dispersed	8.2	10.9	17.2	22.7

* partially flocculated (pH 10.5)